Can dynamically downscaled windstorm footprints be improved by observations through a probabilistic approach?

Article

Published Version

AGU PUBLICATIONS

JGR

Journal of Geophysical Research: Atmospheres

RESEARCH ARTICLE
10.1002/2013JD020882

Key Points:
- We introduced an approach to adjust RCM windstorm footprints to observations
- The method is generally able to enhance the results of dynamical downscaling
- The application of the approach produces better results for wind than for gusts

Supporting Information:
- Readme
- Figure S1
- Figure S2
- Figure S3
- Figure S4

Correspondence to:
R. Haas,
rhaas@meteo.uni-koeln.de

Citation:
Haas, R., J. G. Pinto, and K. Born (2014), Can dynamically downscaled windstorm footprints be improved by observations through a probabilistic approach?, *J. Geophys. Res. Atmos.*, *119*, 713–725, doi:10.1002/2013JD020882.

Received 13 SEP 2013
Accepted 30 DEC 2013
Accepted article online 5 JAN 2014
Published online 31 JAN 2014

Can dynamically downscaled windstorm footprints be improved by observations through a probabilistic approach?

Rabea Haas[1], Joaquim G. Pinto[1,2], and Kai Born[1,3]

[1]Institute for Geophysics and Meteorology, University of Cologne, Cologne, Germany, [2]Department of Meteorology, University of Reading, Reading, UK, [3]TÜV Rheinland Energie und Umwelt GmbH, Cologne, Germany

Abstract Windstorms are a main feature of the European climate and exert strong socioeconomic impacts. Large effort has been made in developing and enhancing models to simulate the intensification of windstorms, resulting footprints, and associated impacts. Simulated wind or gust speeds usually differ from observations, as regional climate models have biases and cannot capture all local effects. An approach to adjust regional climate model (RCM) simulations of wind and wind gust toward observations is introduced. For this purpose, 100 windstorms are selected and observations of 173 (111) test sites of the German Weather Service are considered for wind (gust) speed. Theoretical Weibull distributions are fitted to observed and simulated wind and gust speeds, and the distribution parameters of the observations are interpolated onto the RCM computational grid. A probability mapping approach is applied to relate the distributions and to correct the modeled footprints. The results are not only achieved for single test sites but for an area-wide regular grid. The approach is validated using root-mean-square errors on event and site basis, documenting that the method is generally able to adjust the RCM output toward observations. For gust speeds, an improvement on 88 of 100 events and at about 64% of the test sites is reached. For wind, 99 of 100 improved events and ~84% improved sites can be obtained. This gives confidence on the potential of the introduced approach for many applications, in particular those considering wind data.

1. Introduction

In recent decades, global circulation models (GCMs) have become commonly used tools to understand physical processes in the climate system [e.g., *Meehl et al*., 2007]. They allow for an assessment of possible representations of past, present, and future climate conditions for different spatial scales and a wide range of temporal scales. However, due to their comparatively coarse resolution, GCMs show deficiencies in representing regional and local climate conditions adequately. To overcome this shortcoming, several downscaling techniques have been developed, which can be roughly grouped into dynamical and statistical methods, or a combination of both (for review see, e.g., *Giorgi and Mearns* [1991], *Hewitson and Crane* [1996], *Wilby and Wigley* [1997], and *Maraun et al.* [2010]). For statistical downscaling, large-scale variables (predictors) are related to local variables (predictands) via statistical transfer functions [e.g., *Wilby et al*., 1998; *Hanssen-Bauer et al*., 2005]. For dynamical downscaling, large-scale reanalyses or GCM data are combined with regional climate models (RCMs) resulting in high-resolution simulations (5–50 km) over a region of interest [*Meehl et al*., 2007; *Christensen et al*., 2007]. Statistical-dynamical downscaling usually combines a weather-typing approach with regional climate model (RCM) modeling [e.g., *Fuentes and Heimann*, 2000; *Pinto et al*., 2010]. These techniques can be used both for the purpose of numerical weather prediction and to determine the response of climate change on local- and regional-scale variables.

A large suite of methods has been developed in recent decades, particularly focusing on temperature and precipitation [e.g., *Wilby and Wigley*, 1997]. Less attention has been paid to other variables like 10 m wind speed and—even less often—to wind gusts, although 10 m wind speed is one of the standard meteorological variables reported by weather stations [*World Meteorological Organization*, 2008]. Research on wind speeds and wind gusts at regional and local scales has focused, e.g., on the development and enhancement of methodologies to estimate gust speeds from wind observations [e.g., *Wieringa*, 1973; *Verkaik*, 2000; *De Rooy and Kok*, 2004]. Not only absolute values but also probability distributions of wind speeds can be estimated by empirical downscaling [e.g., *Pryor et al*., 2005; *Pryor and Barthelmie*, 2010]. Further, modeling approaches including wind

gust parameterizations have been developed to obtain wind gust speeds and windstorm footprints comparable to observations [e.g., *Brasseur*, 2001; *Goyette et al*., 2001; *Ágústsson and Ólafsson*, 2009; *Pinto et al*., 2009; *Born et al*., 2012]. However, dynamically downscaled wind or gust speeds do not necessarily match to observations perfectly due to local-scale factors that can affect the measurements and which cannot be captured by the RCMs [e.g., *Goyette et al*., 2003; *Born et al*., 2012].

To bridge this gap, methods to adjust the RCM output toward local observations have been developed. The statistical estimation of the local distribution of a climate variable, when only its large-scale value is given, is known as the climate inversion problem [*Kim et al*., 1984]. Classical approaches usually correct model output at test site locations and were first used in the context of weather forecasts [*Glahn and Lowry*, 1972]. With this aim, the basic methodologies are the "perfect prog" approach and the Model Output Statistics (MOS) approach, which differ in the way of establishing the relationships between the variables [*Klein and Glahn*, 1974]. In the perfect prog approach, the relationship is built between observed predictands and predictors, while in the MOS approach it is built between the predictands and numerical model output. In both approaches, the resulting statistical function is applied to the simulated output.

Although approaches have been developed to obtain results on a regular grid using MOS [e.g., *Glahn et al*., 2009], most MOS applications on wind aim for information only at specific locations [e.g., *Thorarinsdottir and Gneiting*, 2010]. By contrast, this study aims at correcting RCM output on a high-resolution grid by probability mapping. The method is applied not only for grid points where observations are available but also for all grid points in the investigation area. Here we focus on Germany, where the German Weather Service provided a dense network of wind and gust measurements. With this aim, the following three-step procedure is proposed: First, theoretical distributions are fitted to observed and simulated wind and gust speeds. Second, the distribution parameters of the observations are interpolated onto the RCM grid. Finally, the distributions of RCM variables are compared to interpolated distributions of observations by probability mapping. This enables an adjustment of the simulated wind and gust speeds toward the measurements. The results are evaluated using standard root-mean-square error (RMSE) skill scores, which also enable the interpretation of the effectiveness of the procedure for wind and gust speeds event based (i.e., errors averaged over all sites for each event) and site based (i.e., errors averaged over all events for each site).

Details on data sources and preparation are given in section 2. In section 3 methods to fit and to interpolate the data, as well as to validate the results, are explained. This section also includes an introduction to circulation weather types, which are used to analyze the potential influence of large-scale atmospheric circulation on the methodology. The results are presented in section 4, in which a difference is made between results on events and results at test sites. The paper finishes with discussion and conclusion.

2. Data

2.1. Selection of Events

The basic data set is a sample of 100 windstorm events with a strong impact on Europe as selected in *Haas and Pinto* [2012]. The selection of these storms resulted from the calculation of a loss-related meteorological index (MI) after *Pinto et al*. [2012]. The index is computed using ERA-Interim reanalysis data [*Dee et al*., 2011] with a resolution of T225 (0.75°× 0.75°). Six-hourly instantaneous wind speeds over Europe (−14.7657°E to 34.4531°E, 32.6315°N to 66.3155°N) are considered. At each grid point, the cubic exceedance of the local 98th gust percentile is calculated (following *Klawa and Ulbrich* [2003]) and afterward the sum over all land grid points within this area is built. All days during the period 1989 to 2010 are ranked according to the MI. Hundred days with the highest MI are selected as set of events, which are represented by 3 day periods around the event. The detailed event list can be found in Table S1 (supporting information). Although the focus of the present study lies only on Germany, the selection of events was kept on a pan-European basis (a) for consistency with *Haas and Pinto* [2012] and (b) as the ultimate aim is the application of the method on the larger investigation area. As there is a very strong overlapping of the top-ranking storms between Europe and Germany (78% for Top 50 and 61% for Top 100), the results would be comparable if the event selection was performed for Germany alone. This results from the fact that most of the selected 100 storms also affect Germany, due to its geographical location in the center of the chosen Europe domain [see *Haas and Pinto*, 2012, Figure S1].

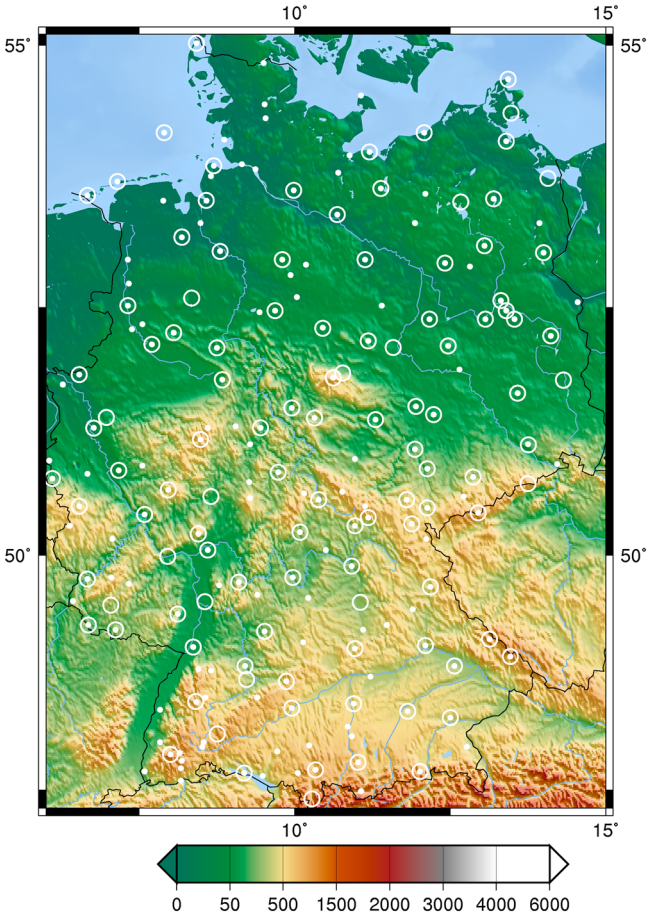

Figure 1. Orography of Germany and locations of test sites, with circles denoting gust measurements and points denoting wind measurements.

2.2. Regional Climate Model

The dynamically downscaled windstorm footprints used in this study are simulations of the COSMO-CLM (RCM of the Consortium for Small-scale Modeling in Climate Mode version 4.8., hereafter CCLM [*Rockel et al.*, 2008]). ERA-Interim reanalysis data are also used as initial and boundary conditions for the simulations of historical storms. By a two-step nesting approach, a resolution of 7 km (0.0625°) is reached. Gust speeds are computed by an approach using friction velocity as estimator for turbulence [*Schulz*, 2008]. A comparison with other wind gust estimation approaches and observations can be found in *Born et al.* [2012]. Both wind and gust speeds are available as RCM output on an hourly basis. Wind speeds are instantaneous values on the hour, while gust speeds are the maxima of all model time steps within the last hour. For the purpose of this study, daily maxima of both parameters are extracted for each RCM grid point. As region of interest, we chose all grid points within the area 5.5°E to 15°E and 47.2°N to 55.1°N (domain including Germany, Figure 1).

2.3. Observations

Wind and gust speed measurements of the observational network of the German Weather Service (DWD) are used. Gust speeds are available as daily maximum and wind speed as hourly mean values, which are aggregated to daily maximum wind speeds if more than 12-hourly values per day are reported. The DWD provides 434 sites measuring wind speed and 299 sites measuring gust speed. However, not all of these sites deliver observations for all of the selected events. For our analyses, 228 sites reported a sufficient amount of wind speed data and 151 sites of gust speed data (reports at minimum 70 of the 100 events). In this context, at least one of the 3 days should have an observation to count the event. Selected test sites should be representative for the surrounding area. Thus, in a second selection step, sites with large outliers differing clearly from neighboring sites are removed resulting in a set of 173 and 111 sites for wind and gusts, respectively

(Figure 1). There is an overlap of 94 test sites measuring both wind and gust speeds (marked with dots and circles in Figure 1). Outliers in observations may originate from steep gradients between two nearby test sites (e.g., the sites around the mountain Brocken; 10.62°E, 51.8°N) or at locations influenced by, e.g., channeling effects or in coastal areas. A distinct increase of the RMSE (>5%) is identified when applying the MOS on the first selection of sites (228 and 151 for wind and gust, respectively).

3. Methodology

In this section, the used methods for data preparation and evaluation are presented. First, the wind data are fitted by theoretical Weibull distributions to determine the parameters. The estimated parameters of observations are interpolated to the RCM grid and related to the parameters of the simulations by a probability mapping. Finally, the results are validated by RMSEs and interpreted using circulation weather types.

3.1. Weibull Fit

For the following calculations, theoretical Weibull distributions are fitted to observed and simulated wind and gust speeds. We consider observations and simulations of the selected events (3 days each, at maximum 300 values in total) to fit the distribution parameters. Several previous studies on wind suggest adopting the Weibull distribution for this purpose (following *Justus et al*. [1978]). The scale parameter α and the shape parameter β can be easily estimated using the cumulative distribution function (CDF) form

$$F(x) = 1 - \exp\left(-\alpha x^{\beta}\right) \tag{1}$$

by replacing α and β with slope m and axis intercept b of a regression line through the wind and gust speeds of each test site or grid point:

$$\ln(-\ln(1 - F(x))) = \ln(\alpha) + \beta \cdot \ln(x) = b + m \cdot \ln(x) \tag{2}$$

Four pairs of parameters are estimated: One pair for wind observations ($m_{\mathrm{Obs,Wind}}$, $b_{\mathrm{Obs,Wind}}$), one pair for gust observations ($m_{\mathrm{Obs,Gust}}$, $b_{\mathrm{Obs,Gust}}$), one pair for wind simulations ($m_{\mathrm{Sim,Wind}}$, $b_{\mathrm{Sim,Wind}}$), and one pair for gust simulations ($m_{\mathrm{Sim,Gust}}$, $b_{\mathrm{Sim,Gust}}$). The correlation between the empirical values and the values resulting from the regression line is on average very high (0.98). Therefore, the uncertainty of the fit is negligible and not further considered. The small deviation of the observations and simulations from the regression line confirms the Weibull distribution to be an appropriate fit. Figure S1 shows an example of transformed wind and gust observations and the regression lines for site Bamberg (Southern Germany).

3.2. Interpolation

To compare observations and simulations, distribution parameters of observations are interpolated to CCLM grid points. Here we use distance-weighted interpolation taking into account the nearest 20 sites to each grid point. The choice of 20 sites was found to be a reasonable compromise between regions with high and low station density. Each of the 20 sites is weighted by a factor w_i, which is calculated using the longitudinal and latitudinal distances in kilometers ($d\mathrm{lon}_i$ and $d\mathrm{lat}_i$) between grid point and sites:

$$w_i = \frac{\exp\left(-\frac{\sqrt{d\mathrm{lon}_i^2 + d\mathrm{lat}_i^2}}{c}\right)}{\sum_{j=1}^{20} \exp\left(-\frac{\sqrt{d\mathrm{lon}_j^2 + d\mathrm{lat}_j^2}}{c}\right)} \tag{3}$$

Here we use a correlation length c of 15 km. This radius has been tested empirically and delivers a good compromise between extreme smoothing and too much details resulting in a patchy interpolated field. The parameters for wind observations ($m_{\mathrm{Obs,Wind}}$, $b_{\mathrm{Obs,Wind}}$) and for gust observations ($m_{\mathrm{Obs,Gust}}$, $b_{\mathrm{Obs,Gust}}$) estimated as stated in the previous section are interpolated using equation (3). In the following, $m_{\mathrm{Obs,Wind}}$, $b_{\mathrm{Obs,Wind}}$, $m_{\mathrm{Obs,Gust}}$, and $b_{\mathrm{Obs,Gust}}$ denote the interpolated parameters, which are needed for the probability mapping.

3.3. Probability Mapping

To adjust the simulated wind and gust speeds (x_{Sim}) to observations (x_{Obs}), a probability mapping is carried out following the quantile-matching method described in *Michelangeli et al.* [2009]. A transfer function is obtained by equalizing the theoretical distributions of observations F_{Obs} and simulations F_{Sim}:

$$F_{Obs}(x_{Obs}) = F_{Sim}(x_{Sim}) \tag{4}$$

As the corrected simulations of wind or gust speeds $x_{Sim,corr}$ are estimations (denoted with the hat) of the observations x_{Obs}, they can be calculated using the inverse distribution of the observations F_{Obs}^{-1} and the distribution of simulations F_{Sim}:

$$x_{Sim,corr} = \widehat{x_{Obs}} = f_{Obs}^{-1}(F_{Sim}(x_{Sim})) = \left(\frac{\ln(1-(1-\exp(-\exp(b_{Sim})\cdot x^{m_{Sim}})))}{-\exp(b_{Obs})}\right)^{\frac{1}{m_{Obs}}} \tag{5}$$

With m_{Obs}, m_{Sim}, b_{Obs}, and b_{Sim} being the estimated slope and axis intercept of the observations and simulations, respectively. The equation can be used for the correction of wind and gust speeds by inserting the according parameters m (slope) and b (intercept).

3.4. Validation

To validate the approach, we compare observed wind and gust speeds x_{Obs} of each event at each site to the uncorrected and corrected simulations x_{Sim} and $x_{Sim,corr}$ of the nearest grid point next to this site. The squared deviations $(x_{Sim} - x_{Obs})^2$ and $(x_{Sim,corr} - x_{Obs})^2$ are each averaged over all events or over all test sites to the root-mean-square error (RMSE) and are normalized with the according means of the observations x_{Obs}. Thus, the relative RMSEs that we use for the following analyses are

$$RMSE_{CCLM} = \frac{\sqrt{\frac{\sum_{i=1}^{n}(x_{Sim}-x_{Obs})2}{n}}}{\frac{\sum_{i=1}^{n}x_{Obs}}{n}} \tag{6a}$$

$$RMSE_{MOS} = \frac{\sqrt{\frac{\sum_{i=1}^{n}(x_{Sim,corr}-x_{Obs})2}{n}}}{\frac{\sum_{i=1}^{n}x_{Obs}}{n}} \tag{6b}$$

Here the number of stations is $n = 173$ for wind speeds and $n = 111$ for gust speeds to evaluate the RMSE score with respect to events. For an evaluation per test site, the score is calculated using n = number of days with observations (with a maximum of 300, 3 days times 100 events).

3.5. Circulation Weather Types

In order to assess the possible influence of large-scale atmospheric circulation on the performance of the methodology, circulation weather types (CWTs) after *Jones et al.* [1993] are calculated. This method is based on the manual Lamb weather types, which were originally used to classify circulation patterns over the British Isles [*Lamb*, 1972; *Jenkinson and Collinson*, 1977], and has been used for many climate variability and climate change studies [e.g., *Buishand and Brandsma*, 1997; *Trigo and DaCamara*, 2000; *Jones et al.*, 2012]. CWTs are determined from geostrophic wind direction and speed using large-scale data of mean sea level pressure (MSLP) at a central point and of 16 surrounding grid points (Figure S2). With this aim, ERA-Interim reanalysis data were interpolated to a 2.5° × 2.5° grid. A central point over Germany (50°N; 10°E) is selected for computations, and the 12 UTC MSLP field is used as representative for the large-scale atmospheric circulation of each day. Following *Jones et al.* [1993], westerly flow, southerly flow, resultant flow, westerly shear vorticity, southerly shear vorticity, and total shear vorticity are determined. Therewith all days are grouped into eight directional types defined as 45° sectors (Figure S3): northeast (NE), east (E), southeast (SE), south (S), southwest (SW), west (W), northwest (NW), and north (N). Additionally, there are two circulation types: cyclonic (C) and anticyclonic (A). If neither rotational nor directional flow dominates, the day is attributed a hybrid CWT (e.g., anticyclonic west). In addition, we also consider the resultant flow parameter f (a measure of

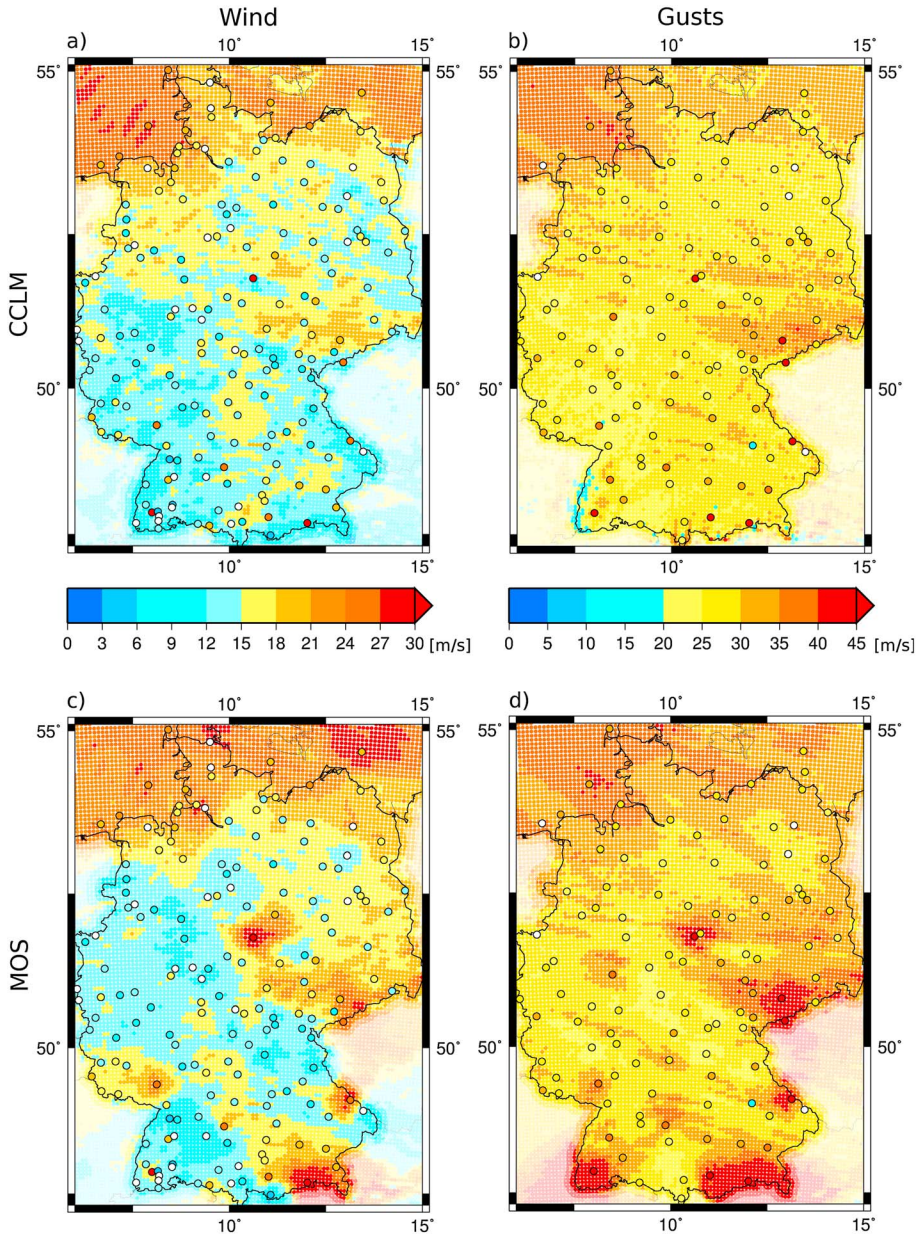

Figure 2. (a and b) Example of originally simulated and (c and d) MOS-corrected footprints. One day signatures of wind (Figures 2a and 2c) and gust speeds (Figures 2b and 2d) for storm Emma (1 March 2008). The black-rimmed dots are the selected test sites, marked in white for missing observations on this date. Neighboring states of Germany are faded out, as no test sites are used in these regions.

intensity of geostrophic wind, calculated from westerly and southerly flow), and its potential influence on the performance of the MOS approach.

4. Results

4.1. Results on Events

In this section, wind and wind gusts derived by the RCM are compared to observations. In particular, their potential improvement by the application of MOS is investigated. The simulated wind and gust speeds are not always congruent with observations, as exemplary shown in Figures 2a and 2b for windstorm Emma (29 February to 2 March 2008). It is apparent that some test sites are overestimated (mainly costal test sites), whereas others are underestimated (mainly at higher altitudes). To reduce this mismatch, the simulated values at the CCLM grid points are corrected according to the transformation equation introduced in section 3.3. After the correction, the

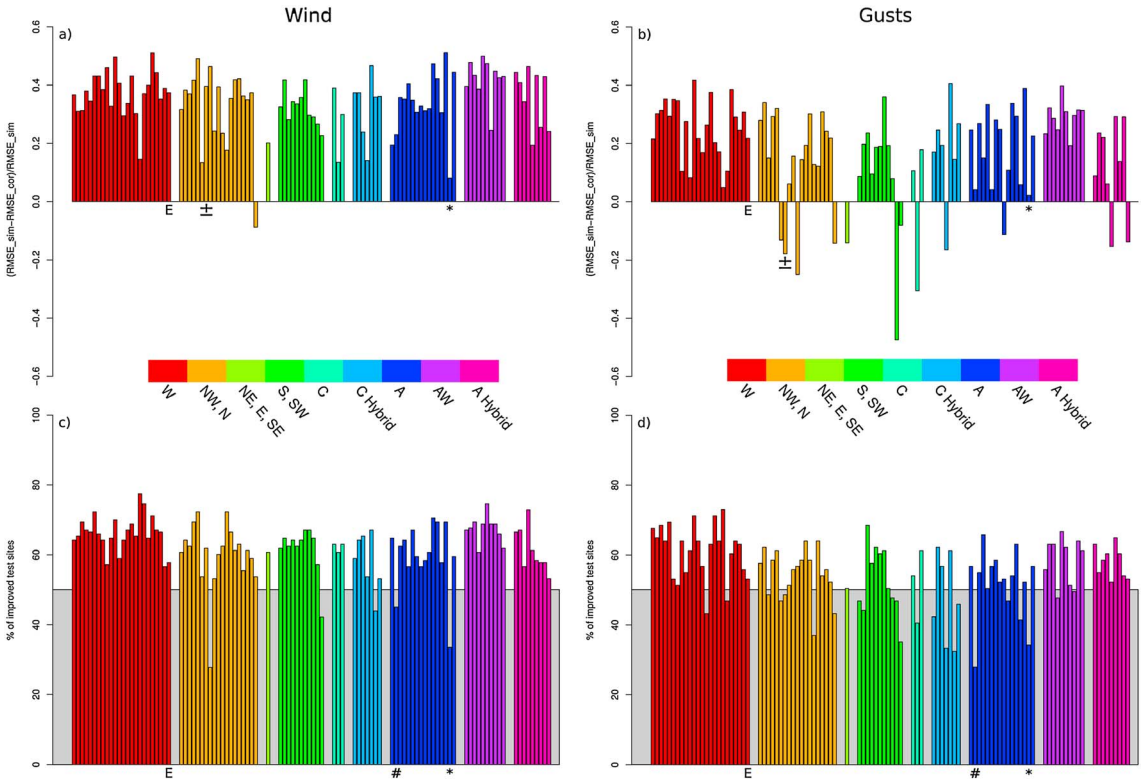

Figure 3. Difference between $RMSE_{CCLM}$ and $RMSE_{MOS}$ for (a) wind and (b) gusts on event basis, with positive values denoting an improvement (decrease of RMSE). Asterisk (5 April 2007) is an example for low improvement without worsening; plus-minus sign (28 March 1995) denotes an example for diverging behavior for wind and gust speeds. Percentage of improved test sites per event regarding (c) wind and (d) gusts: sharp sign (29 January 1989) and asterisk (5 April 2007) denote examples for little number of improved test sites for wind and gust speeds. Bars outside the grey box denote events with more than 50% improved test sites. Events are grouped in CWTs and in chronological order within these groups. Windstorm Emma (1 March 2008) is marked with "E."

spatial patterns of the resulting footprints are in better agreement with observations (Figures 2c and 2d) than the direct RCM output (Figures 2a and 2b). Nevertheless, a small worsening is identified for certain areas, meaning that the MOS correction leads to values further away from observations (overcorrection). This can, e.g., be the case if the original CCLM simulations are already in a very good agreement with the observations.

To give an objective measure of this improvement, the observations are compared to simulations. For each test site, the corresponding nearest neighbor RCM grid point is considered. The deviations at all test sites are summed to calculate two RMSE per event, one for the original simulations ($RMSE_{CCLM}$) and one for the corrected simulations ($RMSE_{MOS}$). For wind speed, the RMSE can be improved on 99 of the 100 events ($RMSE_{CCLM} > RMSE_{MOS}$, Figure 3a). The analysis with gust speeds evidences an improvement on 88 events (Figure 3b). The example of Emma shows a good improvement for both parameters, i.e., the $RMSE_{CCLM}$ summed over all test sites is reduced by the application of the MOS (marked with E in Figure 3). For other events, the approach does not impair the footprints and also does not affect both wind and gust considerably as, e.g., event on 5 April 2007 (denoted with asterisk in Figures 3a and 3b). This small improvement results from quite large event-specific $RMSE_{CCLM}$ (0.4751 for wind and 0.2122 for gusts) that cannot be improved significantly. Compared to Emma, this windstorm produced weaker wind gusts over Germany and caused little damage. This leads to the assumption that the correction may be more effective for higher wind and gust speeds. On the other hand, there are also events, which show a mixed response: while wind speeds are explicitly improved, gust speeds experience a worsening (e.g., event on 28 March 1995, denoted with plus-minus sign in Figures 3a and 3b). As the simulated gusts are already quite good compared to wind speeds, there is a limited potential for improvement, but the risk of an overcorrection. This shows that the change of the RMSE of wind speeds and gusts is not always in agreement.

The influence of the large-scale atmospheric flow conditions on the performance of the methodology is analyzed by assigning CWTs to the 100 windstorm events. With this aim, the CWT type attributed to the middle day of each 3 day period per event is considered. The bars in Figure 3 are colored according to the CWTs, with infrequent types merged together into groups (compare Table 1). In general terms, the improvement due

Table 1. $RMSE_{CCLM}$ and $RMSE_{MOS}$ per CWT[a]

		$RMSE_{CCLM}$		$RMSE_{MOS}$		$(RMSE_{CCLM} - RMSE_{MOS})/RMSE_{CCLM}$	
CWT	Number of Days	Wind	Gust	Wind	Gust	Wind	Gust
West	71	0.3664	0.2580	0.2379	0.2022	**0.3507**	**0.2164**
Northwest, Nord	50	0.3782	0.2549	0.2509	0.2315	0.3366	0.0918
Northeast, east, southeast	3	0.4440	0.2737	0.3395	0.2691	0.2354	0.0168
South, southwest	28	0.3948	0.2603	0.2632	0.2233	0.3335	0.1419
Cyclonic	11	0.4490	0.2986	0.3530	0.3032	0.2137	−0.0157
Cyclonic hybrid	17	0.4303	0.3071	0.3285	0.2910	0.2365	0.0523
Anticyclonic	55	0.4389	0.2882	0.3073	0.2554	0.2999	0.1136
Anticyclonic west	35	0.3727	0.2420	0.2295	0.1849	**0.3843**	**0.2357**
Anticyclonic hybrid (excluding anticyclonic west)	30	0.3896	0.2384	0.2448	0.2018	**0.3715**	0.1537
All	300	0.3930	0.2661	0.2620	0.2252	0.3333	0.1535

[a]Outstanding low and large improvements for wind (below 25% and above 35%) and gusts (below 10% and above 20%) are underlined and marked in bold, respectively.

to MOS is somewhat dependent on the CWT. Exceptions are events occurring during infrequent CWTs (NE/E/S; C; C hybrid), for which the improvement of the RMSE is small in the case of wind and gust speed. These improvements below 10% for gusts and 25% for wind are marked as underlined values in Table 1. On the other hand, the best improvements (>20%, bold values in Table 1) for gust speeds are found for west or anticyclonic west CWT events. This is in line with the above statement that the MOS has a stronger influence on larger gust speeds, as intense windstorms are often associated with westerly weather situations [*Donat et al.*, 2010]. The same CWTs contribute to the best RMSE improvements regarding wind speed, with the anticyclonic hybrid type additionally featuring improvements above 35%. The overall view points to a better behavior of the methodology for wind than for gusts with an averaged enhancement of ~33% and ~15%, respectively.

In addition to the RMSE, Figures 3c and 3d depict the percentage of improved test sites per event. The percentage of improved test sites for wind speed (Figure 3c) is generally higher than for gust speeds (Figure 3d). For wind speed, almost all events (95 of 100) show an improvement for more than 50% of the test sites. On the other hand, the application of the MOS on gust speeds does not deliver such clear results (77 of 100 events above 50%). For some events, the percentage of improved test sides falls below the 50% line in both data sets (e.g., 29 January 1989 or 5 April 2007; marked with sharp sign and asterisk in Figures 3c and 3d). These events are characterized by comparatively weak wind and gust speeds over Germany, so this finding corroborates the idea that the applied MOS improvement performs better on stronger events.

4.2. Results at Test Sites

We now consider how far the MOS application leads to an improvement of the results at individual test sites. When summing up the deviations over all events, for 145 of the 173 test sites (83.82%), $RMSE_{MOS}$ is smaller than $RMSE_{CCLM}$. These improved test sites have a homogeneous spatial distribution over Germany without any clear spots or highlighted regions (Figure 4a). Figure 4c shows that for most of the test sites, where the MOS application increases the RMSE, the change is only marginal with negative values close to zero. For gust speeds, the $RMSE_{CCLM}$ is reduced at 71 of 111 test sites, which corresponds to 63.96%. The spatial pattern is comparable to the one of the wind speeds (Figure 4b), but with a tendency to smaller RMSE changes with a clear peak in the histogram around zero (Figure 4d). The outliers (<−0.3), both in the wind and the gusts histograms (Figures 4c and 4d), can be attributed to local effects like steep topographical gradients.

A detailed analysis at each of the test sites leads to the conclusion that they can be separated into three categories: At test sites of the first category, most events are improved by the MOS, if CCLM wind and gust speeds are larger than observed values (Figures 5a–5d). This is the case if most of the cumulative distribution function (CDF) of the simulations lies below the CDF of the observations (Figures 5e and 5f). These test sites can be identified by

$$\mu + 0.5 \cdot \sigma < x \ \wedge \ m_{Obs} < m_{CCLM} \ \wedge \ b_{Obs} > b_{CCLM},$$
$$\text{or} \quad \mu - 0.5 \cdot \sigma > x \ \wedge \ m_{Obs} > m_{CCLM}.$$

with x being the intersection of the two CDFs with the distribution parameters m_{Obs}, m_{CCLM}, b_{Obs}, and b_{CCLM}, μ is the mean of the observations of the 100 events and σ is the corresponding standard deviation. The interval $[\mu - 0.5 \cdot \sigma; \mu + 0.5]$ has been selected after empirical tests.

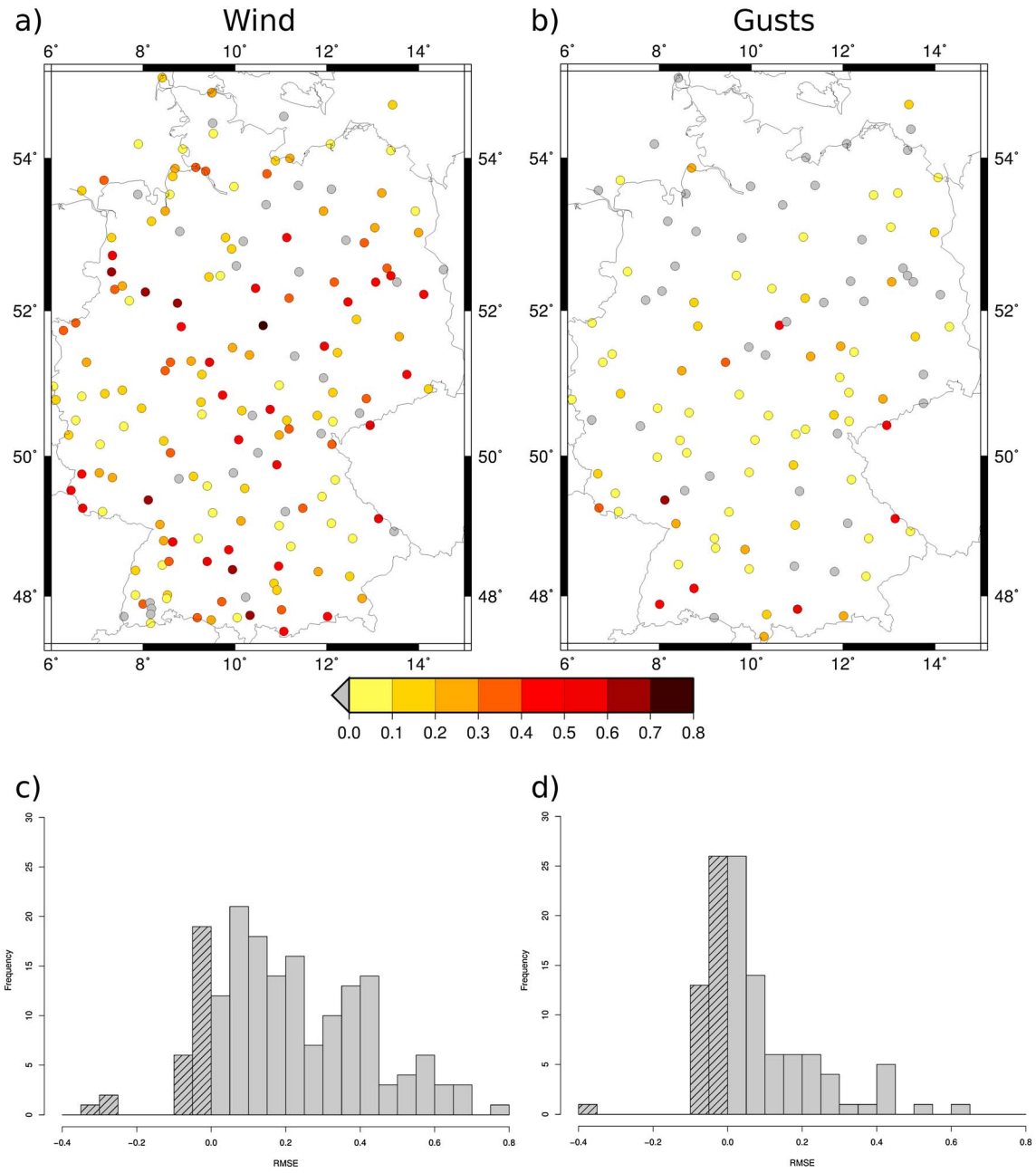

Figure 4. Spatial distribution of (a) 173 test sites selected for wind and (b) 111 test sites selected for gusts. Colors according to change in RMSE between original and corrected simulation normalized with the RMSE of the original simulation. Histogram of improvement (positive values) and disimprovement (negative values, shaded, corresponding to grey dots in Figures 4a and 4b) test sites for (c) wind and (d) gusts.

For category 2, the MOS improves events with simulated wind or gust speeds being smaller than the observed (Figures 6a–6d). These test sites can be identified by a CDF of CCLM values above the CDF of measurements (Figures 6e and 6f). An objective identification scheme would be

$$\mu + 0.5 \cdot \sigma < x \wedge m_{\mathrm{Obs}} > m_{\mathrm{CCLM}} \wedge b_{\mathrm{Obs}} < b_{\mathrm{CCLM}},$$
$$\text{or } \mu - 0.5 \cdot \sigma > x \wedge m_{\mathrm{Obs}} < m_{\mathrm{CCLM}}.$$

For the third category, it is difficult to apply the MOS, because the events are widely scattered (rare category, Figure S4). This category is characterized by intersecting CDFs near the mean of the observations ($\mu - 0.5 \cdot \sigma < x < \mu + 0.5 \cdot \sigma$). Ninety-four test sites report wind and wind gusts (marked with dots and circles in Figure 1), whereof at 64 sites the sorting lead to the same category regarding wind or gusts.

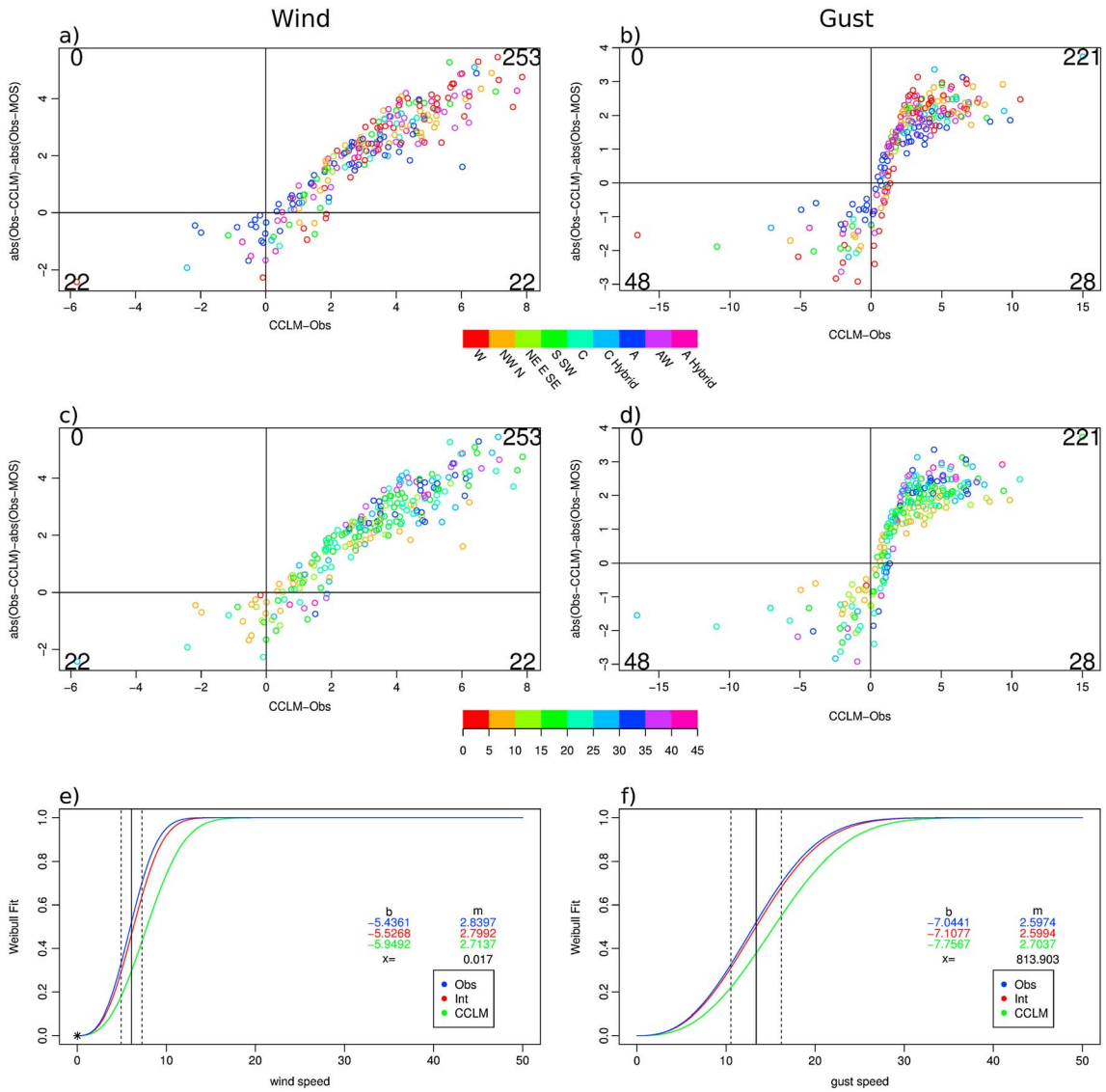

Figure 5. Category 1: Events are improved if CCLM > observation. (Dis)improvement of the simulations by the MOS against difference between original simulation and observation. Colors are according to (a and b) CWTs and (c and d) *f* parameter. The numbers denote the number of events in each corner (maximal sum = 300). (e and f) Distribution of observations (blue), interpolated distribution of observations (red), and distribution of simulations (green). Solid vertical line is the mean (μ) of the observations, and dashed vertical lines build the interval $[\mu - 0.5 \cdot \sigma; \mu + 0.5 \cdot \sigma]$ with the standard deviation σ. (left) Wind and (right) gusts.

On the one hand, observations could be interpolated to grid points as absolute values to identify whether the simulated gust or wind speed is greater than the observation on grid point basis. On the other hand, this would result in large uncertainties. In order to find an alternative method to identify the events for which $RMSE_{MOS}$ is larger than $RMSE_{CCLM}$, the dependence on the CWT of each event is examined. The dots in Figures 5a, 5b, 6a, and 6b are colored according to the CWT for each event. For the shown categories 1 and 2, there is apparently little correlation between CWT and an improvement of the $RMSE_{CCLM}$. Especially for gusts, at most category 3 test sites (Figure S4), the events with an anticyclonic CWT are distributed like events at category 1 test sites, i.e., scattered around a diagonal from bottom left to top right (c.f. Figures 5a–5d). They are corrected, if the CCLM value is larger than the observation. In contrast, the distribution of events with a westerly CWT tends to be more comparable to events at category 2 test sites, as they are improved if the CCLM value is smaller than the observation, corresponding to a diagonal from top left to bottom right (c.f. Figures 6a–6d). Thus, the consideration of the CWT can potentially help to interpret the scattering of the events and to refine the classification of categories. Nevertheless, further considerations would be necessary to effectively use the CWT information in practical terms.

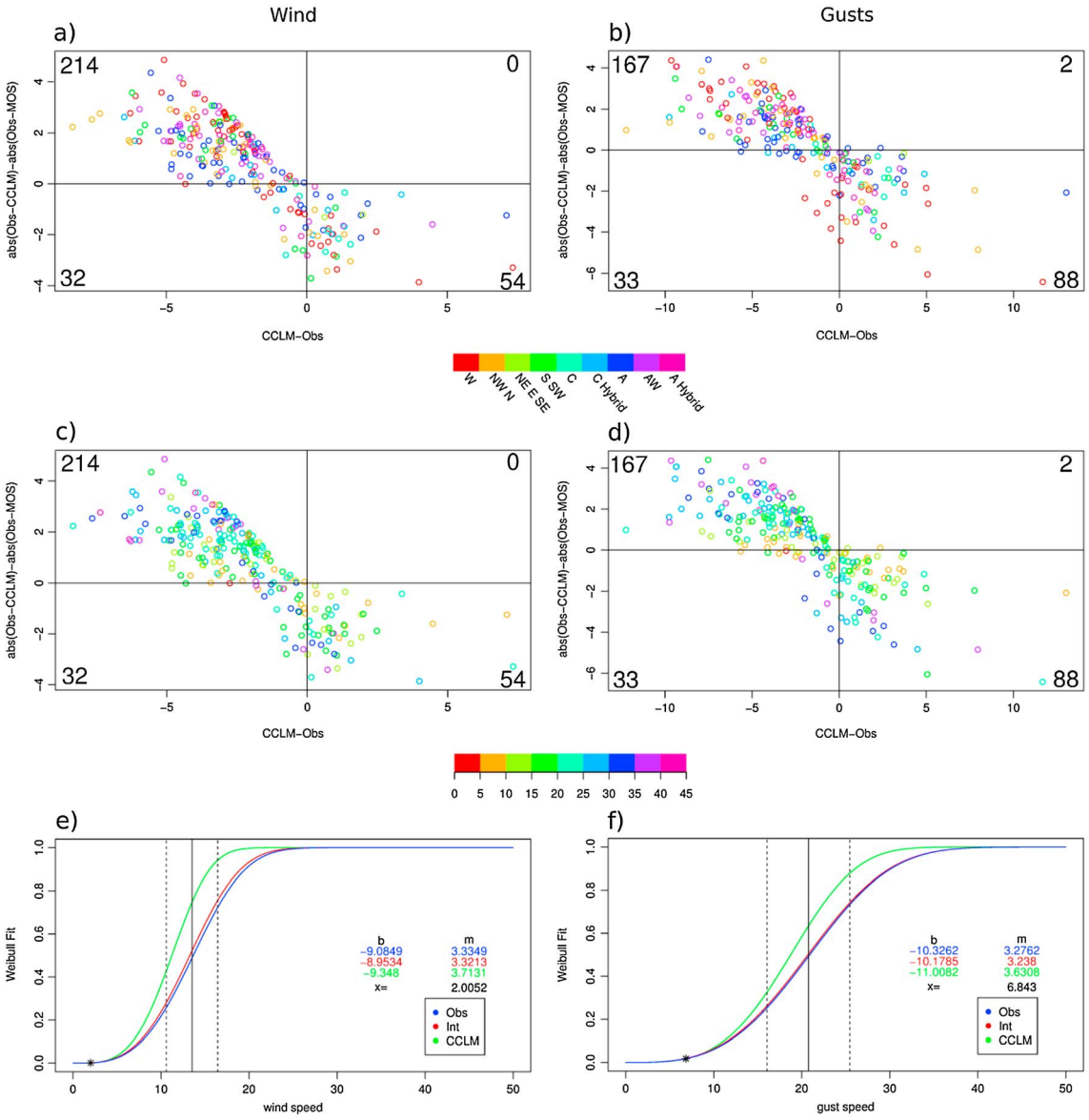

Figure 6. Category 2: Events are improved if CCLM < observation. As in Figure 5.

The CWT classification not only reflects the direction of the large-scale circulation but also provides *f* as measure of the total geostrophic flow intensity induced by the synoptic situation. The dots in Figures 5c, 5d, 6c, and 6d are colored according to this parameter. At category 1 and 2 test sites, the events with small *f* parameters tend to be little affected by the MOS, while events with large *f* parameters show a clear adjustment either in positive or negative direction. This is attributed to the fact that high wind and gust speeds can be attributed to large *f* values, thus having more potential to be adjusted by the approach. At category 3 test sites, events with small *f* values tend to behave as events at category 1 test sites, thus being corrected if the CCLM value is larger than the observation (analogue to category 3 and CWT types). Accordingly, events with large *f* values tend to behave as events at category 2 test sites, thus being improved if the CCLM value is smaller than the observation.

In general, a reasonable improvement of wind speeds by the use of the MOS approach is found. The RMSE summed over all events and test sites is decreased by 33% (Table 1). The application on gusts also brings an overall improvement (15%, Table 1) but has more outliers for specific events or test sites.

5. Discussion and Conclusions

In this study, we introduced an approach to adjust dynamically downscaled windstorm footprints to observations. For this purpose, we selected 100 storm events, which had a large impact on Europe and compared wind and gust speeds simulated by the CCLM with according observations of 173 (111) DWD test sites. At each grid point and each test site the theoretical Weibull distribution is fitted to wind and gust speeds. The distributions of observations are interpolated to the CCLM grid points to use both distributions in a probability mapping approach to correct the simulated values. Unlike most previous studies dealing with MOS applied on wind data, we developed and applied the method not only for specific locations as, e.g., wind farms, but for producing an area-wide output on a grid. It has been shown that this method is generally able to enhance the results of dynamical downscaling toward observations. Nevertheless, when considering gust speeds, there are still some events and test sites that are not improved, or in some cases even worsened. By contrast, the application of the approach on wind speeds clearly produces better results, both event and site based.

The analysis of events indicated an improvement of 99% for wind speed and 88% for gust speed. Thereby, events having a pronounced wind signature with high wind or gust speeds have a larger potential to be corrected by the introduced MOS approach. However, we found that the change in RMSE for wind and the change in RMSE for gusts are not always congruent. The analysis of test sites also delivers better results for wind speeds (~84% improved sites) than for gust speeds (~64% improved sites). The quality of the MOS application on test site basis can be quantified by an objective scheme regarding the deviation between observations and simulations of the closest grid point. To get the information at each grid point, such an identification of categories could also be based on the CDF of the interpolated distribution parameters.

In general terms, an application of this methodology to wind speed can be recommended due to the promising improvement of the wind fields. On the other hand, the methodology should be further improved before it can generally be applied to wind gust data, as currently less improvement is found. The generally better performance of the approach applied on wind speed in comparison to gust speed can be attributed to several reasons. First, it is presumably due to the strong temporal variability of gusts and the local differences. This also involves more extremes and outliers in the gust data. Second, the larger data sets for hourly wind speed may play a determinant role on the enhanced performance of the approach. Longer time series of gust speeds with a sufficient number of observations at more sites would potentially bring the results for gust closer to the ones for wind.

Future investigations should focus on a larger domain (Europe) to be able to adjust the full downscaling model introduced in *Haas and Pinto* [2012], provided an adequate set of measurement data is available. Eventually, the interpolation scheme needs to be adapted to be applicable on a larger set of test sites. This could, e.g., be done by adjusting the weighting factors or by embedding local characteristics like topography to avoid too steep gradients in the interpolated field. The effective use of the CWT information to identify events or test sites with a large or small potential of correction still needs further considerations. The use of historical data delivers the opportunity to apply an event-based MOS or the objective identification scheme introduced in section 4.2 to enhance the results for gust speeds. Such an identification of generally good or worse performing events or test sites is, due to the obvious nonexistence of observations for the future, not applicable for future climate investigations. Nevertheless, without this identification, the MOS approach itself can be applied for future climate investigations, if the transfer functions for wind and gust speed are assumed to be stationary in time. This assumption of stationarity should be proofed in future studies. Regarding the promising results for wind speed, a clear potential for application on GCM simulations is evident. The approach could, e.g., be applied in combination with the downscaling method introduced in *Haas and Pinto* [2012]. This enables the analysis of decadal predictability and climate change projections considering large ensembles. The methodology could also be applied to other variables like temperature, for which much better data coverage exists.

Acknowledgments
We thank the ECMWF for the ERA-Interim Reanalysis data set and the DWD for providing the wind and gust speed data. This research was supported by the German Federal Ministry of Education and Research (BMBF) under the project Probabilistic Decadal Forecast for Central and Western Europe(MIKLIP-PRODEF, contract 01LP1120A). We thank P. Ludwig, M.K. Karremann, and J. Mömken for help with data processing and CLM simulations. We also thank three anonymous reviewers for their helpful and constructive comments.

References

Ágústsson, H., and H. Ólafsson (2009), Forecasting wind gusts in complex terrain, *Meteorol. Atmos. Phys.*, *103*, 173–185.
Born, K., P. Ludwig, and J. G. Pinto (2012), Wind gust estimation for Mid-European winter storms: Towards a probabilistic view, *Tellus A*, *64*, 17,471, doi:10.3402/tellusa.v64i0.17471.
Brasseur, O. (2001), Development and application of a physical approach to estimating wind gusts, *Mon. Weather Rev.*, *129*, 5–25.

Buishand, A., and T. Brandsma (1997), Comparison of circulation classification schemes for predicting temperature and precipitation in the Netherlands, *Int. J. Climatol.*, *17*, 875–889.
Christensen, J., et al. (2007), Regional climate projections, in *Climate Change, 2007: The Physical Science Basis, Contribution of Working Group I to the Fourth Assessment Report of the Intergovernmental Panel on Climate Change*, chap. 11, pp. 847–940, Cambridge Univ. Press, Cambridge.
De Rooy, W. C., and K. Kok (2004), A combined physical-statistical approach for the downscaling of model wind speed, *Wea. Forecast.*, *19*, 485–495.
Dee, D. P., et al. (2011), The ERA-Interim reanalysis: Configuration and performance of the data assimilation system, *Q. J. R. Meteorol. Soc.*, *137*, 553–597.
Donat, M. G., G. C. Leckebusch, J. G. Pinto, and U. Ulbrich (2010), Examination of wind storms over Central Europe with respect to circulation weather types and NAO phases, *Int. J. Climatol.*, *30*, 1289–1300, doi:10.1002/joc.1982.
Fuentes, U., and D. Heimann (2000), An improved statistical-dynamical downscaling scheme and its application to the alpine precipitation climatology, *Theor. Appl. Climatol.*, *65*, 119–135.
Giorgi, F., and L. O. Mearns (1991), Approaches to the simulation of regional climate changes: A review, *Rev. Geophys.*, *29*, 191–216.
Glahn, H. R., and D. A. Lowry (1972), The use of Model Output Statistics (MOS) in objective weather forecasting, *J. Appl. Meteorol.*, *11*, 1203–1211.
Glahn, B., K. Gilbert, R. Cosgrove, D. P. Ruth, and K. Sheets (2009), The gridding of MOS, *Wea. Forecast.*, *24*, 520–529.
Goyette, S., M. Beniston, D. Caya, J. P. R. Laprise, and P. Jungo (2001), Numerical investigation of an extreme storm with the Canadian Regional Climate Model: The case study of windstorm VIVIAN, Switzerland, February 27, 1990, *Clim. Dyn.*, *18*, 145–178, doi:10.1007/s003820100166.
Goyette, S., O. Brasseur, and M. Beniston (2003), Application of a new wind gust parameterization: Multiscale case studies performed with the Canadian regional climate model, *J. Geophys. Res.*, *108*(D134374), doi:10.1029/2002JD002646.
Haas, R., and J. G. Pinto (2012), A combined statistical and dynamical approach for downscaling large-scale footprints of European windstorms, *Geophys. Res. Lett.*, *39*, L23804, doi:10.1029/2012GL054014.
Hanssen-Bauer, I., C. Achberger, R. E. Benestad, D. Chen, and E. J. Førland (2005), Statistical downscaling of climate scenarios over Scandinavia, *Clim. Res.*, *29*, 255–268.
Hewitson, B. C., and R. G. Crane (1996), Climate downscaling: Techniques and application, *Clim. Res.*, *7*, 85–95.
Jenkinson, A. F., and F. P. Collinson (1977), An initial climatology of gales over the North Sea, Synoptic Climatology Branch Memorandum, 62, Met. Office, Bracknell, U. K.
Jones, P. D., M. Hulme, and K. R. Briffa (1993), A comparison of Lamb circulation types with an objective classification scheme, *Int. J. Climatol.*, *13*, 655–663, doi:10.1002/joc.3370130606.
Jones, P. D., C. Harpham, and K. R. Briffa (2012), Lamb weather types derived from reanalysis products, *Int. J. Climatol.*, *33*, 1129–1139, doi:10.1002/joc.3498.
Justus, C. G., W. R. Hargraves, A. Mikhail, and D. Graber (1978), Methods for estimating wind speed distributions, *J. Appl. Meteorol.*, *17*, 350–353.
Kim, J.-W., J.-T. Chang, N. L. Baker, D. S. Wilks, and W. L. Gates (1984), The statistical problem of climate inversion: Determination of the relationship between local and large-scale climate, *Mon. Weather Rev.*, *112*, 2069–2077.
Klawa, M., and U. Ulbrich (2003), A model for the estimation of storm losses and the identification of severe winter storms in Germany, *Nat. Hazards Earth Syst. Sci.*, *3*, 725–732.
Klein, W. H., and H. R. Glahn (1974), Forecasting local weather by means of Model Output Statistics, *Bull. Am. Meteorol. Soc.*, *55*, 1217–1227.
Lamb, H. H. (1972), *British Isles Weather Types and a Register of the Daily Sequence of Circulation Patterns 1981–1971*, Geophys. Mem., vol. 116, p. 85, HMSO, London.
Maraun, D., et al. (2010), Precipitation downscaling under climate change: Recent developments to bridge the gap between dynamical models and the end user, *Rev. Geophys.*, *48*, RG3003, doi:10.1029/2009RG000314.
Meehl, G. A., et al. (2007), Global climate projections, in *Climate Change 2007: The Physical Science Basis. Contribution of Working Group I to the Fourth Assessment Report of the Intergovernmental Panel on Climate Change*, pp. 747–845, Cambridge Univ. Press, U. K.
Michelangeli, P.-A., M. Vrac, and H. Loukos (2009), Probabilistic downscaling approaches: Application to wind cumulative distribution functions, *Geophys. Res. Lett.*, *36*, L11708, doi:10.1029/2009GL038401.
Pinto, J. G., C. P. Neuhaus, A. Krüger, and M. Kerschgens (2009), Assessment of the wind gust estimates method in mesoscale modelling of storm events over West Germany, *Meteorol. Z.*, *18*, 495–506.
Pinto, J. G., C. P. Neuhaus, G. C. Leckebusch, M. Reyers, and M. Kerschgens (2010), Estimation of wind storm impacts over West Germany under future climate conditions using a statistical-dynamical downscaling approach, *Tellus A*, *62*, 188–201.
Pinto, J. G., M. K. Karremann, K. Born, P. M. Della-Marta, and M. Klawa (2012), Loss potentials associated with European windstorms under future climate conditions, *Clim. Res.*, *54*, 1–20.
Pryor, S. C., and R. J. Barthelmie (2010), Climate change impacts on wind energy: A review, *Renew. Sust. Energy Rev.*, *14*, 430–437.
Pryor, S. C., J. T. Schoof, and R. J. Barthelmie (2005), Empirical downscaling of wind speed probability distributions, *J. Geophys. Res.*, *110*, D19109, doi:10.1029/2005JD005899.
Rockel, B., A. Will, and A. Hense (2008), The regional climate model COSMO-CLM (CCLM), *Meteorol. Z.*, *17*, 347–348.
Schulz, J. P. (2008), Revision of the turbulent gust diagnostics in the COSMO model, *COSMO Newsl.*, *8*, 17–22.
Thorarinsdottir, T. L., and T. Gneiting (2010), Probabilistic forecasts of wind speed: Ensemble Model Output Statistics by using heteroscedastic censored regression, *J. R. Statist. Soc. Series A*, *173*, 371–388.
Trigo, R. M., and C. C. DaCamara (2000), Circulation weather types and their influence on the precipitation regime in Portugal, *Int. J. Climatol.*, *20*, 1559–1581.
Verkaik, J. W. (2000), Evaluation of two gustiness models for exposure correction calculations, *J. Appl. Meteorol.*, *39*, 1613–1626.
Wieringa, J. (1973), Gust factors over open water and built-up country, *Boundary Layer Meteorol.*, *3*, 424–441.
Wilby, R. L., and T. M. L. Wigley (1997), Downscaling general circulation model output: A review of methods and limitations, *Prog. Phys. Geogr.*, *21*, 530–548.
Wilby, R. L., T. M. L. Wigley, D. Conway, P. D. Jones, B. C. Hewitson, and D. S. Wilks (1998), Statistical downscaling of GCM output: A comparison of methods, *Water Resour. Res.*, *34*, 2995–3008.
World Meteorological Organization (WMO) (2008), Guide to meteorological instruments and methods of observation, WMO-No. 8, WMO, Geneva, Switzerland.